

# Slow Scintillation Component and Radiation Induced Readout Noise in Pure CsI Crystals

Fan Yang, *Member*, Liyuan Zhang, *Member*, Ren-Yuan Zhu, *Senior Member, IEEE*

**Abstract**— Because of its fast decay time and low cost, pure CsI crystals are used in HEP experiments for fast crystal calorimetry. CsI crystal samples from three vendors were characterized for the Mu2e experiment at Fermilab with data used to define crystal specification. In addition to the fast scintillation component peaked at 310 nm, a slow scintillation component peaked at 450 nm with  $\mu\text{s}$  decay time was detected, which may be eliminated spectroscopically by using optical filters. It was also found that the slow scintillation component and the radiation induced readout noise in CsI crystals are highly correlated. The nature of the slow scintillation component is believed to be defects and/or impurity related.

## I. SLOW SCINTILLATION IN CSI

CESIUM iodide (CsI) crystal is one of the most cost effective fast crystal scintillators received much attention recently. To measure electron candidates of 106 MeV to 5% precision, the Mu2e-I experiment is building a fast crystal calorimeter by using pure CsI crystals featured with fast scintillation of 30 ns decay time and good radiation resistance up to 10 krad [1-8]. Pure CsI crystals have a potential to be used for fast crystal calorimetry in future HEP experiments in the intensity frontier.

In this paper we discuss two crucial issues for pure CsI application in HEP experiments: slow scintillation component and radiation induced readout noise. Seven samples from three vendors are used in this investigation. Two Kharkov samples are of  $2.9 \times 2.9 \times 23 \text{ cm}^3$ . An Optomaterial sample is of  $3 \times 3 \times 20 \text{ cm}^3$ . Four SICCAS samples are of  $3 \times 3 \times 20$  and  $3.4 \times 3.4 \times 20 \text{ cm}^3$ . Fig. 1 shows a summary of their light output (LO) in 200 ns gate (top), FWHM energy resolution (ER) for Na-22  $\gamma$ -rays (middle) and light response uniformity (LRU) (bottom), which is defined as the rms of the LO values measured at seven points along the crystal. Also shown in the plots are the Mu2e specifications (pink dashed lines). It is clear that most samples satisfy the specifications, indicating crystal growth technique for pure CsI is mature.

Fig. 2 shows light output as a function of integration gate for three crystals from different vendors. In addition to the fast scintillation component of  $\sim 30$  ns decay time CsI crystals show increased LO for increased integration gate width, indicating a sample-dependent slow scintillation component with decay time of a few  $\mu\text{s}$ , which would cause harmful pileup effect so need to be controlled to an appropriate level.

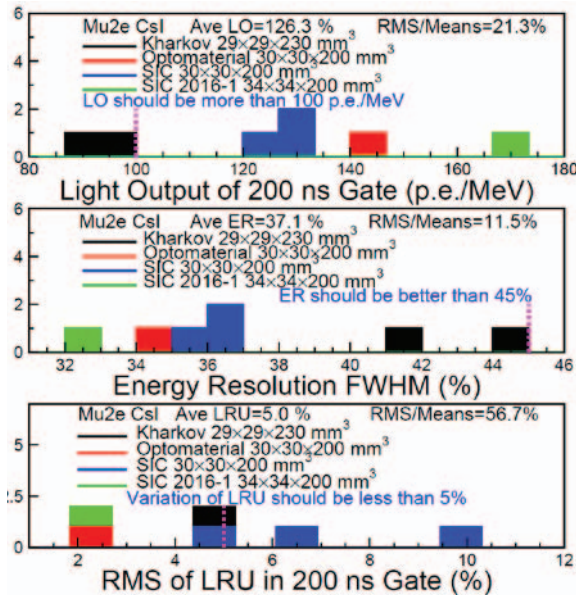


Fig. 1 Summary of the light output in 200 ns gate (top), the FWHM energy resolution of Na-22 peak (middle) and the light response uniformity in 200 ns gate (bottom) for pure CsI crystals from three vendors. Also shown in the plots are the corresponding Mu2e specifications (pink dashed lines).

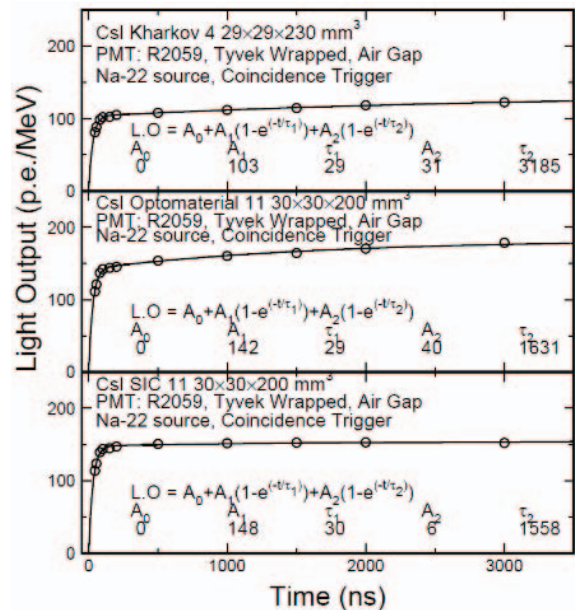


Fig. 2 Light output is shown as a function of the integration gate for CsI crystal samples from three vendors.

Manuscript received December 10, 2016. This work is supported by the U.S. Department of Energy, Office of High Energy Physics program under Award Number DE-SC0011925.

Fan Yang, Liyuan Zhang and Renyuan Zhu are with the California Institute of Technology, Pasadena, CA 91125, USA

The top three plots of Fig. 3 show LO values measured at seven points evenly distributed along the crystal axis with 100, 200 and 3,000 ns gate respectively for the sample Kharkov 4. The corresponding rms values is defined as the LRU. The bottom plot of Fig. 4 shows the Fast/Total (F/T) ratios for 100 and 200 ns gate versus 3000 ns gate. The average F/T ratio of these seven points is 73% and 75% respectively for this sample, indicating significant slow scintillation.

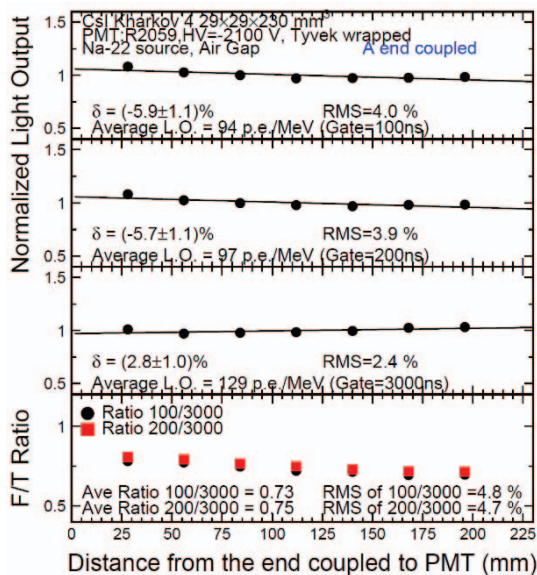


Fig. 3 LO (top three) and F/T ratio (bottom) measured at seven points with 100, 200 and 3000 ns gate, and 100 and 200 ns versus 3000 ns.

Fig. 4 summarizes the F/T ratio of LO(200)/LO(3000) for all samples, where the CsI crystals from SIC show the best F/T ratio. We also found that the sample SIC 6 has no slow scintillation component, indicating that the slow scintillation component may be eliminated by optimizing crystal growth.

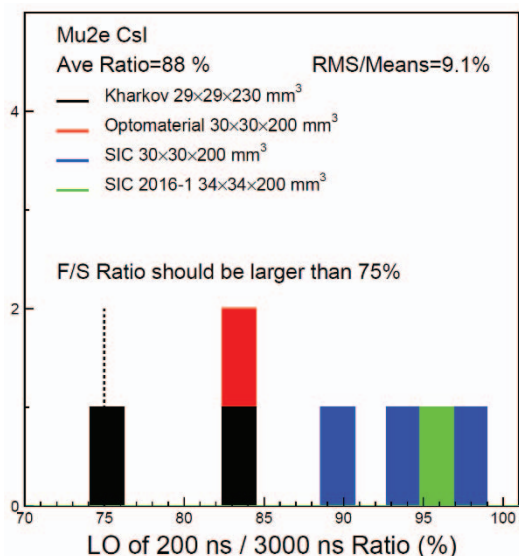


Fig. 4 Summary of the F/T ratio of LO(200 ns)/LO(3000 ns).

Fig. 5 compares X-ray excited luminescence (XEL) spectra for SIC 6 (red), which has no slow component, and Kharkov 4

(blue), which has high slow component. An additional emission peak at 450 nm is clearly observed in Kharkov 4, which is suspected to cause the slow scintillation. Also shown in Fig. 5 is the band width between 275 and 375 nm for a FGUV-11 band pass filter which fits well the intrinsic fast emission peak at 310 nm in CsI crystals.

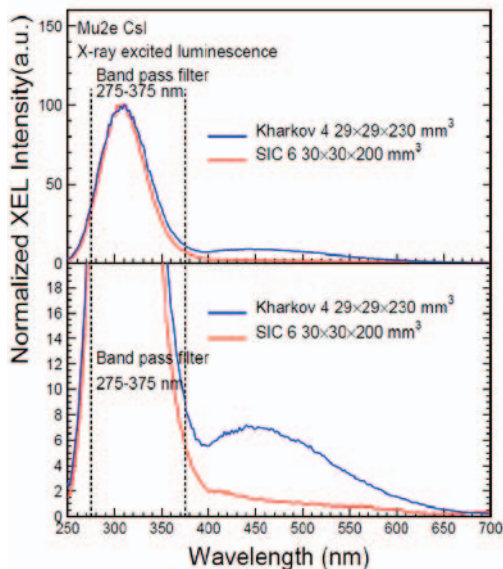


Fig.5 XEL spectra (top) and their expanded view (bottom) for CsI samples with different level of slow component and the FGUV-11 filter.

Fig.6. shows LO as a function of integration gate for three CsI samples with (red) and without (black) a FGUV-11 filter inserted between the sample and PMT. It is clear that the FGUV-11 filter eliminated slow scintillation component in all samples, confirming that the slow scintillation component is caused by the emission peaked at 450 nm, which can be eliminated by such a band pass filter.

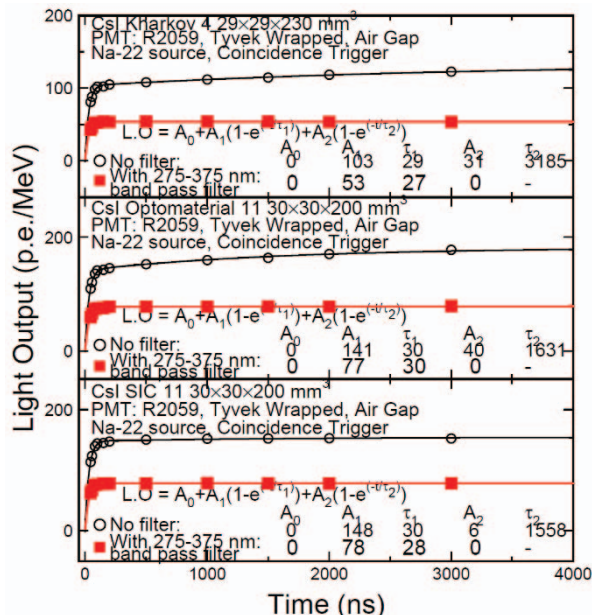


Fig. 6 Light output is shown as a function of the integration gate for CsI samples from three vendors with and without FGUV-11 filter.



## II. RADIATION INDUCED PHOTOCURRENT AND READOUT NOISE IN CSI CRYSTALS

The radiation environment in the hottest region of the Mu2e experiment is 10 krad/year ionization dose and  $2 \times 10^{11}$  n/cm<sup>2</sup>/year neutron fluence with a three times safety factor. Assuming 230 days run per year ( $2 \times 10^7$  sec), the radiation in the hottest region is 1.8 rad/h for ionization dose and  $1 \times 10^4$  n/cm<sup>2</sup>/s for neutrons.

We extract  $\gamma$ -ray and neutron induced energy equivalent readout noise ( $\sigma$ ) as the standard deviation of the photoelectron number ( $Q$ ) in the readout gate:

$$\frac{\sqrt{Q}}{LO} \text{ MeV} \quad (1)$$

We also define  $F$  as radiation induced photoelectron numbers per second, determined by measuring the anode current in PMT.

$$F = \frac{\text{Photocurrent}}{\text{Dose rate}_{\gamma\text{-ray or Flux}_{\text{neutron}}} \times \text{Gain}_{\text{PMT}}} \quad (2)$$

Fig. 7 shows a comparison of the anode current, measured before, during and after irradiation at a dose rate of 2 rad/h for three CsI crystal samples from different vendors, which have slow scintillation component. The decay of the  $\gamma$ -ray induced afterglow was fitted well with three time constants: 0.8, 4.7 and 22.8 hours.

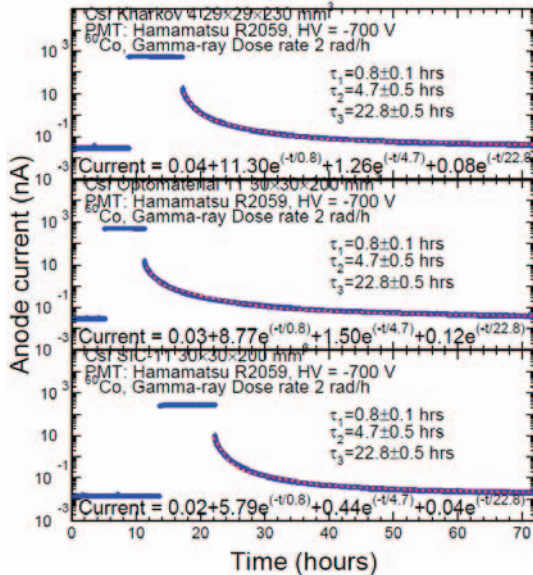


Fig. 7 History of photocurrent measured before, during and after  $\gamma$ -ray irradiation for three CsI samples with slow scintillation component

Fig. 8 shows a comparison of the anode current, measured before, during and after irradiation at a dose rate of 2 rad/h for the sample SIC 6 which has no slow scintillation component. The decay of  $\gamma$ -ray induced afterglow can be fitted to two time constants of 0.4 and 3.0 hours, indicating that the slow time constant of 22.8 hours in the samples shown in Fig. 7 is related

to the slow scintillation. Eliminating the slow scintillation thus should also eliminate this long decay afterglow.

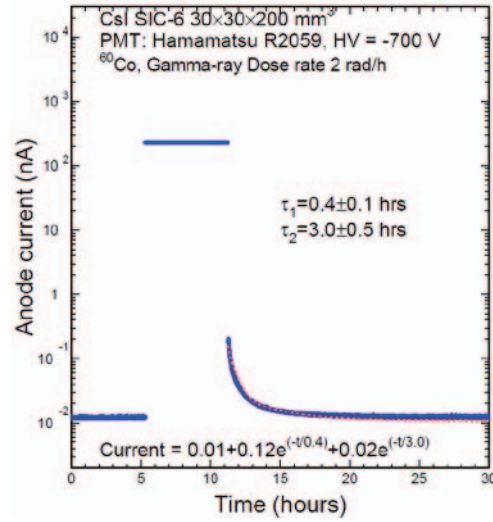


Fig. 8 History of photocurrent measured before, during and after  $\gamma$ -ray irradiation for one CsI sample without slow scintillation component

Fig. 9 shows the history of photocurrent measured before, during and after neutron irradiation for two crystal samples Kharkov 3 and SIC 14. While the sample Kharkov 3 has slow scintillation component, the sample SIC 14 does not. The decay of neutron induced afterglow in Kharkov 3 was fitted to three time constants while that of SIC 14 was fitted to two time constants, confirming that the long decay time of the Cf-252 induced afterglow is also correlated to the slow scintillation component in the CsI crystals. We also notice that the two time constants of the neutron induced afterglow are consistent with that induced by  $\gamma$ -rays, indicating that the radiation induced photocurrent in neutron irradiated samples is caused by the associated  $\gamma$ -rays from the Cf-252 source.

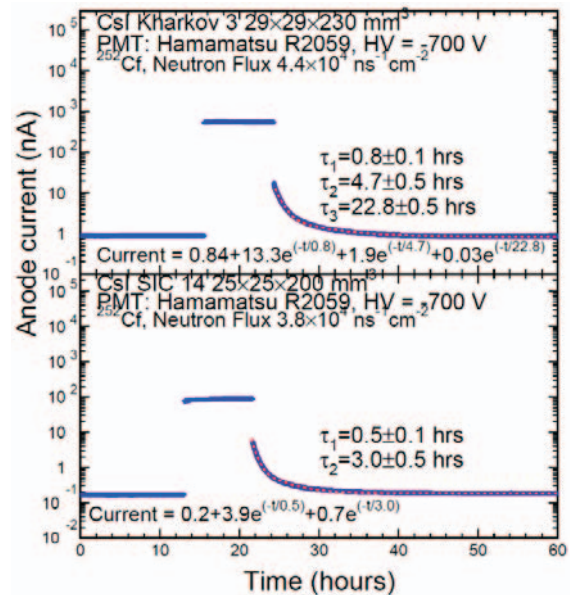


Fig.9 History of photocurrent measured for two CsI samples with (top) and without (bottom) slow scintillation component.

Table 1 and 2 show the energy equivalent readout noise ( $\sigma$ ) induced by  $\gamma$ -rays and neutrons respectively in CsI crystals, where the dark current, radiation induced photocurrent, F and  $\sigma$  were normalized to the Mu2e CsI dimension of  $3.4 \times 3.4 \times 20$  cm<sup>3</sup>. It is clear that the readout noises induced by both  $\gamma$ -rays and neutrons are much smaller than 1 MeV, required by the Mu2e experiment. We also notice that the readout noise induced by  $\gamma$ -rays is much larger than that from neutrons even with  $\gamma$ -ray background. CsI quality control on this aspect can thus be carried out on ionization dose only.

Table 1 Gamma-ray Induced Readout Noise in CsI Crystals under 1.8 rad/h

Sample	Dimensions (cm <sup>3</sup> )	LO of 200 ns Gate (p.e./MeV)	Dark Current (nA)*	Photo current @2 rad/h (nA)*	F (p.e./s/rad/hr)*	$\sigma$ (MeV)*
Kharkov 4	2.9×2.9×23	96	0.035	679	6.68E+09	5.11E-01
Opto 11	3×3×20	140	0.039	663	6.53E+09	3.46E-01
SIC 6	3×3×20	125	0.015	296	2.91E+09	2.59E-01
SIC 11	3×3×20	128	0.018	330	3.25E+09	2.67E-01
SIC 13	3×3×20	130	0.026	461	4.54E+09	3.11E-01

Table 2 Neutron Induced Noise in CsI Crystals under  $1 \times 10^4$  n/cm<sup>2</sup>/s

Sample	Dimensions (cm <sup>3</sup> )	LO of 200 ns Gate (p.e./MeV)	Dark Current (nA)*	Photo current (nA)*	F (p.e./n/cm <sup>2</sup> )*	$\sigma$ (MeV)*
Kharkov 3	2.9×2.9×23	88	0.08	112	5.01E+04	1.1E-01
SIC 2014	2.5×2.5×20	140	0.013	165	8.68E+04	9.4E-02

Fig. 10 shows excellent correlations at a level of 90% and 94% respectively between the volume normalized dark current (top) and the  $\gamma$ -ray induced readout noise (bottom) versus the F/T ratio, where crystal volume was normalized to  $3.4 \times 3.4 \times 20$  cm<sup>3</sup>. This observation indicates that both dark current and  $\gamma$ -ray induced readout noise have the same origin as the slow scintillation component.

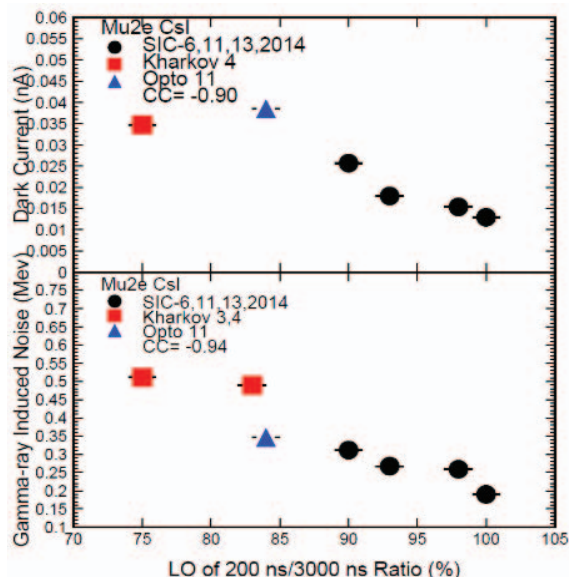


Fig. 10 Correlations between the dark current and the  $\gamma$ -ray induced readout noise versus the F/T ratio.

### III. SUMMARY

The Mu2e experiment at Fermilab is constructing a fast crystal calorimeter using pure CsI crystals. Seven CsI crystals from commercial vendors were characterized with data used to define crystal specifications. We observed a slow scintillation component peaked at 450 nm with  $\mu$ s decay time in most of these samples, which is believed to be defects or impurity related. By inserting an optical band-pass filter between the crystal and the photodetector this slow component may be eliminated spectroscopically. A specification on the F/T ratio of LO(200 ns)/LO(3000 ns) is defined to make sure that the pileup effect caused by the slow component is under control. Advanced R&D on CsI crystals would help to reduce the slow component.

Gamma-ray and neutron induced photocurrent and afterglow were measured for CsI crystals, and was used to extract radiation induced readout noise for the ionization dose rate and neutron flux expected by Mu2e. The latter is found to be much less than the Mu2e requirement of 1 MeV. Excellent correlations have been observed between the dark current and the  $\gamma$ -ray induced readout noise versus the F/T ratio, indicating they are of the same origin. Efforts on eliminating the slow scintillation component thus will also help to reduce dark current and radiation induced readout noise.

### ACKNOWLEDGEMENTS

The authors are grateful to the Mu2e colleagues in the calorimeter group for the CsI samples discussed in this paper and many useful discussions.

### REFERENCES

- [1] M. Angelucci, M. Cestelli Guidi, P. Ciambriano, F. Colao, M. Cordelli, E. Dane, *et al.*, "The MU2E experiment at Fermilab," [http://www.lnf.infn.it/rapatt/2015/pmu2e\\_2016\\_misc.pdf](http://www.lnf.infn.it/rapatt/2015/pmu2e_2016_misc.pdf).
- [2] F. Yang, L. Zhang, and R. Y. Zhu, "Gamma-Ray Induced Radiation Damage Up to 340Mrad in Various Scintillation Crystals," *IEEE T Nucl Sci*, vol. 63, pp. 612-619, 2016.
- [3] R. Y. Zhu, "Precision crystal calorimetry in future high energy colliders," *IEEE T Nucl Sci*, vol. 44, pp. 468-476, Jun 1997.
- [4] Z. Y. Wei and R. Y. Zhu, "A Study on Undoped Csi Crystals," *Nucl Instrum Meth A*, vol. 326, pp. 508-512, Mar 10 1993.
- [5] R. Y. Zhu, "Radiation damage in scintillating crystals," *Nucl Instrum Meth A*, vol. 413, pp. 297-311, Aug 21 1998.
- [6] R. Y. Zhu, "Precision crystal calorimetry in high energy physics," *Nuclear Physics B - Proceedings Supplements*, vol. 78, pp. 203-219, August 1999.
- [7] N. Atanov, V. Baranov, J. Budagov, R. Carosi, F. Cervelli, F. Colao, *et al.*, "Design and status of the Mu2e electromagnetic calorimeter," *Nucl Instrum Meth A*, vol. 824, pp. 695-698, 7/11/ 2016.
- [8] J. Budagov, R. Carosi, F. Cervelli, C. Cheng, M. Cordelli, Y. Davydov, *et al.*, "The calorimeter project for the Mu2e experiment," *Nucl Instrum Meth A*, vol. 718, pp. 56-59, 8/1/ 2013.